

Thermoelectric properties of icosahedral quasicrystals: A phenomenological approach

Enrique Maciá^{a)}

*GISC, Departamento de Física de Materiales, Facultad de Físicas, Universidad Complutense,
E-28040 Madrid, Spain*

(Received 3 September 2002; accepted 27 October 2002)

In this work, we introduce a phenomenological model describing the thermoelectric power of icosahedral quasicrystals. On the basis of a realistic model for the spectral conductivity, obtained from *ab initio* band-structure calculations [C. Landauro and H. Solbrig, *Physica B* **301**, 267 (2000)], we derive a closed analytical expression for the Seebeck coefficient, satisfactorily describing its temperature dependence $S(T)$ over a wide temperature range. We introduce four phenomenological coefficients relating the electronic structure to characteristic features of the experimental $S(T)$ curves. By comparing our analytical results with available experimental data we relate the sensitivity of the thermopower curve to minor variations in the chemical composition to a systematic shift of the Fermi-level position. © 2003 American Institute of Physics.
[DOI: 10.1063/1.1530358]

I. INTRODUCTION

Following the attainment of thermodynamically stable quasicrystals (QC's) of high-structural quality,¹ an increasing number of transport measurements have been performed. By comparing the obtained data with the transport properties of conventional alloys of similar composition, several anomalous behaviors in the temperature and composition dependences of electrical conductivity, Hall coefficient, thermal conductivity, and thermoelectric power have been reported.^{2–8} In this way, it has been progressively realized that QC's occupy an odd position among the well-ordered condensed-matter phases. In fact, on the one hand, most transport properties resemble a more semiconductorlike than metallic character.^{9–11} On the other hand, typical metallic fingerprints, like the presence of a well-defined Fermi edge¹² or an ideal ohmic behavior over a broad voltage range,¹³ have been observed in high-quality icosahedral samples. In addition, it has been theoretically suggested that Wiedemann–Franz's law should also be followed by QC's.¹⁴ Therefore, neither the notion of metal nor that of semiconductor seem to be suitable for QC's, clearly requiring the introduction of a more adequate concept.

Nevertheless, a proper classification of QC's able to encompass the peculiarities of their electronic structure and their unusual transport properties within a unifying conceptual scheme remains still elusive. The puzzle includes the basic fundamental question concerning whether the purported transport anomalies should be mainly attributed to the characteristic quasiperiodic order of QC's or, alternatively, the very nature of the chemical bonding in these materials plays a major role in determining their physical properties. Two recent works have contributed to substantiate this issue by studying the influence of quasiperiodicity on the transport properties of an hypothetical decagonal aluminum QC,¹⁵ or

the role of hybridization mechanisms in the cohesion of cubic approximants in the i -Cd(Ca, Yb) family.¹⁶ It seems reasonable, however, that a definite answer may require a proper combination of both kinds of contributions, so that both long-range quasiperiodicity effects and local atomic environment effects should be considered all together.^{17,18} Promising evidence in this sense comes from experimental and theoretical works showing that the structural evolution from the amorphous to the quasicrystalline state is accompanied by a parallel evolution of the electronic transport anomalies.¹⁹

In previous works we have considered simplified models for the electronic density of states (DOS) of icosahedral QC's in order to estimate the influence of their electronic structure on the transport coefficients.^{20–22} The aim of this work is to introduce a *phenomenological model* relating several topological features observed in the thermoelectric power curves, like extrema or sign reversals, with the main features of the electronic structure of QC's. To this end, we shall consider the spectral conductivity model proposed by Landauro and Solbrig (LS). This model was obtained from *ab initio* band-structure calculations.^{23,24} On the basis of the LS model we will perform a detailed analytical study, deriving a *closed analytical expression* for the Seebeck coefficient. The obtained function satisfactorily describes its temperature dependence $S(T)$ over a wide temperature range. In this way, we will introduce a number of *phenomenological coefficients*, analytically relating the electronic structure to some characteristic topological features observed in the experimental thermopower curves. In addition, by comparing the theoretical $S(T)$ curves obtained from our analytical treatment with pertinent experimental data for icosahedral QC's of different compositions, we will relate the purported sensitivity of the $S(T)$ curves to minor variations in the chemical composition to a systematic shift of the Fermi-level position of the considered samples.

The paper is organized as follows. In Sec. II, we briefly review relevant experimental results concerning the thermo-

^{a)}Electronic mail: macia@material.fis.ucm.es

electric power of QC's. In Sec. III, we describe the main features of the LS model for the spectral conductivity. In Sec. IV, we introduce our phenomenological model and obtain closed analytical expressions describing the temperature dependence of the Seebeck coefficient. Section V is devoted to compare the obtained analytical results with suitable experimental data, highlighting the physical implications of the phenomenological coefficients previously introduced. Finally, in Sec. VI, we summarize the main conclusions of this work.

II. THERMOELECTRIC POWER OF ICOSAHEDRAL QUASICRYSTALS

During the last decade, the thermoelectric power of samples belonging to different icosahedral families has been measured.^{25–40} Reported data refer to a broad range of stoichiometric compositions and cover different temperature ranges in the interval from 1 to 900 K. From the collected data the following general conclusions can be drawn. First, the thermoelectric power usually exhibits large values when compared to those of both crystalline and disordered metallic systems.⁴¹ Second, the temperature dependence of the Seebeck coefficient usually deviates from the linear behavior, exhibiting pronounced curvatures (either positive or negative) at temperatures above ~ 50 – 100 K. This behavior is at variance with that exhibited by ordinary metallic alloys where the $S(T)$ curve is dominated by electron diffusion yielding a linear temperature dependence. Third, small variations in the chemical composition (of just a few atomic percent) can give rise to sign reversals in the thermopower value. Fourth, the $S(T)$ curves exhibit well-defined extrema in several cases. For example, high-quality samples belonging to the system i -AlCu(Fe,Ru) show $S(T)$ well-defined extrema in the temperature range 80 – 250 K.^{26–31} The presence of broad maxima has been recently observed in high-quality i -AlPd(Mn,Re) samples at temperatures above ~ 500 K.^{37,38,42} Both the magnitude and position of these extrema are extremely sensitive to minor variations in the chemical stoichiometry of the sample. Fifth, for a given sample stoichiometry, the thermopower shows a strong dependence on the annealing conditions induced onto the sample during the synthesis process.^{30,33,34} Finally, significant differences among the $S(T)$ curves corresponding to poly-grained and single-grained i -AlPdRe samples have been observed.^{34,43}

Most of the anomalous behaviors listed above are mainly observed in high-quality QC's containing transition metals. In fact, it was reported that poor quality, metastable QC phases containing only simple and noble metals, like i -AlCuMg,²⁵ obey a linear relation of the type $S(T) \sim aT$. In addition, the order of magnitude of their thermopower is typical of metallic alloys ($|S| \lesssim 10 \mu\text{V K}^{-1}$) over the entire temperature range considered. On the other hand, thermopower measurements of rare-earth bearing QC's in the system i -ZnMg(Y,Tb,Ho,Er) also exhibit markedly linear temperature dependences of S above ~ 50 K, with slopes ranging from approximately 0.015 to $0.030 \mu\text{V K}^{-2}$.³⁹ An analogous behavior has been reported for the thermodynamically stable CdYb QC, which also contains rare-earth

atoms.⁴⁰ Such different behaviors among the i -AlCu(Fe,Ru,Os) and i -AlPd(Mn,Re) families (bearing transition metals) and the i -ZnMg(RE) and i -CdYb families (bearing rare-earth atoms), strongly suggest that chemical effects may be playing a significant role.

III. ELECTRONIC STRUCTURE MODEL

Our study will focus on the relationship between the conductivity spectrum, $\sigma(E)$, defined as the $T \rightarrow 0$ conductivity with the Fermi level at energy E , and the transport properties. Generally speaking the conductivity spectrum should take into account both band-structure effects and those effects related to the critical nature of the electronic states.^{20,44} In fact, although it may be tempting to assume that the $\sigma(E)$ function should closely resemble the overall structure of the DOS, it has been shown that a dip in the $\sigma(E)$ curve can correspond to a peak in the DOS at certain energies.^{23,24,45} This behavior is likely to be related to the peculiar nature of critical electronic states.^{45–47} In fact, according to the expression $\sigma(E) \propto N(E)D(E)$, the conductivity spectrum depends on the diffusivity of the electronic states, $D(E)$, as well as on the DOS structure $N(E)$. Concerning the DOS structure, most efforts aimed to understand the unusual transport phenomena of QC's have focused on the existence of a pronounced pseudogap at the Fermi level,^{48–54} and the possible presence of a dense set of nested peaks in the DOS.^{55,56} The physical origin of such peaks may stem from the structural quasiperiodicity of the substrate via a hierarchical cluster aggregation resonance,⁵⁷ or through d -orbital resonance effects.⁵⁸ At the time being, however, the very existence of such peaks remains controversial.^{59–65} In any event, in order to make a meaningful comparison between experimental measurements and numerical results, one should take into account possible phason, finite lifetime, and temperature broadening effects. In so doing, it is observed that most finer details in the DOS are significantly smeared out, and only the most conspicuous peaks remain in the vicinity of the Fermi level at room temperature.¹² These considerations convey us to reduce the number of main spectral features necessary to capture the most relevant physics of the transport processes. Two fruitful approaches have been recently considered in the literature to this end. On the one hand, the *ab initio* study performed by Landauro and Solbrig has shown that the spectral resistivity $\rho(E)$ corresponding to i -AlCuFe phases, can be satisfactorily modeled by means of just two basic spectral features, namely, a wide and a narrow Lorentzian peaks.²³ Quite remarkably, this model is able to properly fit the experimental $\sigma(T)$ and $S(T)$ curves in a broad temperature range.²⁴ Following a different line of reasoning, aimed to encompass the transport properties of both amorphous phases and QC's within a unified scheme, Häussler and collaborators have shown that the main qualitative features of the $\sigma(T)$, $S(T)$, as well as the Hall coefficient curves, can be accounted for by considering an *asymmetric* spectral conductivity function characterized by a broad minimum (arising from a momentum-based spherical resonance mechanism) exhibiting a pronounced dip within it (due to

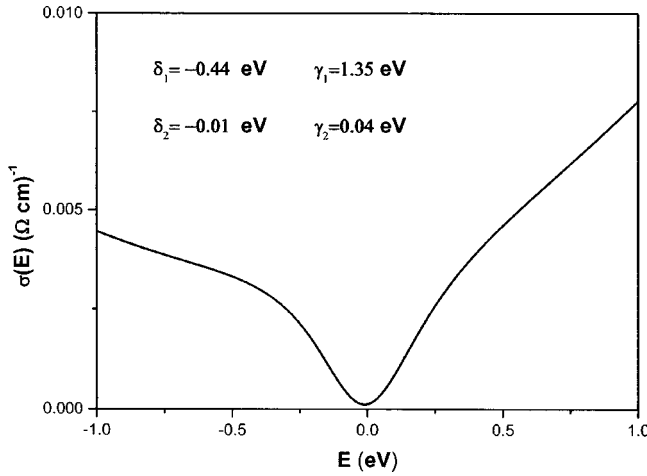


FIG. 1. Spectral conductivity curve in the energy interval ± 1 eV around the Fermi level as obtained from Eq. (1) for the electronic model parameter values γ_i and δ_i indicated in the frame.

angular or planar order, based on an angular momentum resonance triggered by a hybridization mechanism).¹⁹

Motivated by these results, in this work we shall start by considering the LS model for the spectral conductivity

$$\sigma(E) \equiv A[L_1(E) + L_2(E)]^{-1}, \quad (1)$$

where the parameter A is expressed in $\Omega^{-1} \text{cm}^{-1} \text{eV}^{-1}$ units and the Lorentzians

$$L_i(E) = \frac{\gamma_i}{\pi} [\gamma_i^2 + (E - \mu - \delta_i)^2]^{-1}, \quad (2)$$

characterize the height ($\pi\gamma_i$)⁻¹ and position δ_i of each spectral feature with reference to the Fermi-level μ . In addition, the γ_i parameters can be related to the diffusivity of the corresponding states.^{66,23} Thus, the variation of the transport properties with the temperature will be determined as a proper combination of both band-structure effects and the critical nature of the electron wave functions in a natural way. For the sake of illustration in Fig. 1 the spectral conductivity curve, as obtained from expression (1), is shown for a suitable choice of the parameters γ_i and δ_i .²³ The overall behavior of this curve agrees well with the experimental results obtained from tunneling and point contact spectroscopy measurements, where the presence of a dip feature of small width superimposed onto a broad, asymmetric pseudogap has been reported.^{62,63}

IV. ANALYTICAL TREATMENT

In this work, the study of the transport properties is based on the energy spectrum function $\sigma(E)$. Then, following previous works^{19–22,24,29} We will start by expressing the Seebeck coefficient in the way

$$S(T) = \frac{1}{e\sigma(T)T} \int_{-\infty}^{+\infty} dE \left(-\frac{\partial f}{\partial E} \right) (E - \mu) \sigma(E), \quad (3)$$

where

$$\sigma(T) = \int_{-\infty}^{+\infty} dE \left(-\frac{\partial f}{\partial E} \right) \sigma(E), \quad (4)$$

is the electrical conductivity, e is the electron charge, T is the temperature, $f(E, T)$ is the Fermi distribution, and E is the electron energy. By expressing Eqs. (3) and (4) in terms of the scaled variable $x \equiv \beta(E - \mu)$, with $\beta \equiv (k_B T)^{-1}$, where k_B is the Boltzmann constant, we get^{21,22}

$$S(T) = \frac{cJ_1}{J_0}, \quad (5)$$

where $c \equiv -k_B/|e| \approx -87 \mu\text{VK}^{-1}$, and we have introduced the integrals

$$J_n(\beta) \equiv \int_{-\infty}^{+\infty} x^n \text{sech}^2(x/2) \sigma(x) dx. \quad (6)$$

Expressing Eq. (1) in terms of the scaled variable as $\sigma(x) = c_0 P_4(x)/P_2(x)$, where

$$P_4(x) \equiv \beta^{-4} x^4 - 2\beta^{-3} n_3 x^3 + \beta^{-2} n_2 x^2 - 2\beta^{-1} n_1 x + n_0, \quad (7)$$

$$P_2(x) \equiv \beta^{-2} x^2 - 2\beta^{-1} q_1 x + q_0,$$

where $c_0 \equiv \pi A (\gamma_1 + \gamma_2)^{-1}$, $n_3 \equiv \delta_1 + \delta_2$, $n_2 \equiv \varepsilon_1^2 + \varepsilon_2^2 + 4\delta_1\delta_2$, $n_1 \equiv \delta_2\varepsilon_1^2 + \delta_1\varepsilon_2^2$, $n_0 \equiv \varepsilon_1^2\varepsilon_2^2$, $q_0 \equiv \varepsilon_1^2\varepsilon_2^2(\gamma_1 + \gamma_2)^{-1}$, $q_1 \equiv (\gamma_1\delta_2 + \delta_1\gamma_2)(\gamma_1 + \gamma_2)^{-1}$, with $\varepsilon_i^2 \equiv \gamma_i^2 + \delta_i^2$, and $\varepsilon \equiv \gamma_1\varepsilon_1^{-2} + \gamma_2\varepsilon_2^{-2}$, we can rewrite Eq. (6) in the form

$$J_n c_0^{-1} = \int_{-\infty}^{\infty} \left[\sum_{k=0}^2 a_k \beta^{-k} x^{n+k} + \frac{Q_{n+1}(x)}{P_2(x)} \right] \text{sech}^2(x/2) dx, \quad (8)$$

where

$$a_0 \equiv 2a_1q_1 + n_2 - q_0$$

$$= \frac{(\gamma_1 + \gamma_2)(\gamma_1\varepsilon_1^2 + \gamma_2\varepsilon_2^2) - 4\gamma_1\gamma_2\Delta\delta^2}{(\gamma_1 + \gamma_2)^2}, \quad (9)$$

$$a_1 \equiv 2(q_1 - n_3) = -2 \frac{\delta_1\gamma_1 + \delta_2\gamma_2}{\gamma_1 + \gamma_2}, \quad a_2 = 1,$$

with $\Delta \equiv \delta_1 - \delta_2$, and $Q_{n+1}(x) \equiv a_3\beta^{-1}x^{n+1} + a_4x^n$, with

$$a_3 \equiv 2a_0q_1 - 2n_1 - a_1q_0$$

$$= -4\gamma_1\gamma_2\Delta\delta \frac{2q_1\Delta\delta - \varepsilon_1^2 + \varepsilon_2^2}{(\gamma_1 + \gamma_2)^2}, \quad (10)$$

$$a_4 \equiv n_0 - a_0q_0$$

$$= \gamma_1\gamma_2 \frac{4\varepsilon_1^2\varepsilon_2^2\Delta\delta^2 - (\varepsilon_1^2 - \varepsilon_2^2)^2(\gamma_1 + \gamma_2)}{(\gamma_1 + \gamma_2)^3}.$$

Making use of the integrals

$$\int_{-\infty}^{\infty} \text{sech}^2(x/2) dx = 4, \quad \int_{-\infty}^{\infty} x^2 \text{sech}^2(x/2) dx = \frac{4\pi^2}{3},$$

$$\int_{-\infty}^{\infty} x^4 \text{sech}^2(x/2) dx = \frac{28\pi^4}{15},$$

$$\int_{-\infty}^{\infty} x^l \text{sech}^2(x/2) dx = 0, \quad (l \text{ odd}),$$

we obtain

$$J_0 c_0^{-1} = 4\pi^2 \beta^{-2} / 3 + a_3 \beta^{-1} H_1 + a_4 H_0 + 4a_0, \tag{11}$$

$$J_1 c_0^{-1} = 4\pi^2 a_1 \beta^{-1} / 3 + a_5 H_1 + a_3 \beta G_0,$$

where

$$a_5 \equiv 2q_1 a_3 + a_4 = -\frac{\gamma_2 \gamma_1 \varepsilon_3}{(\gamma_1 + \gamma_2)^4} [(\gamma_1 - \gamma_2)^2 (\varepsilon_3 + 4\Delta \delta^2) + 4\Delta \delta (\delta_2 \gamma_2^2 - \delta_1 \gamma_1^2)], \tag{12}$$

with $\varepsilon_3 \equiv (\gamma_1 + \gamma_2)^2 + \Delta \delta^2$, $G_0 \equiv 4 - q_0 H_0$, and we have introduced the auxiliary integrals

$$H_k(\beta) \equiv \int_{-\infty}^{\infty} \frac{x^k}{P_2(x)} \operatorname{sech}^2(x/2) dx. \tag{13}$$

In order to evaluate these integrals we shall expand the function $P_2^{-1}(x)$ in Taylor series around the Fermi level to get

$$H_0 \approx \frac{4}{q_0} \left(1 + \frac{\pi^2}{3} \frac{4q_1^2 - q_0}{q_0^2} \beta^{-2} \right),$$

$$H_1 \approx \frac{8\pi^2 q_1 \beta^{-1}}{3q_0^2} \left(1 + \frac{14\pi^2}{5} \frac{2q_1^2 - q_0}{q_0^2} \beta^{-2} \right). \tag{14}$$

By plugging Eqs. (14) into Eqs. (11) and (5), keeping $O(\beta^{-4})$ terms, we finally arrive to the following expression for the Seebeck coefficient:

$$S(T) = -2|e| \mathcal{L}_0 T \mathcal{F}(T), \tag{15}$$

where $\mathcal{L}_0 = \pi^2 k_B^2 / 3e^2 = 2.44 \times 10^{-8} \text{ V}^2 \text{ K}^{-2}$ is the Lorenz number and we have introduced the auxiliary function

$$\mathcal{F}(T) = \frac{\xi_1 + \xi_3 b T^2}{1 + \xi_2 b T^2 + \xi_4 b^2 T^4}, \tag{16}$$

where $b \equiv e^2 \mathcal{L}_0 = 2.44 \times 10^{-8} \text{ (eV)}^2 \text{ K}^{-2}$, and

$$\xi_1 \equiv -\frac{\gamma_1 \delta_1 \varepsilon_2^4 + \gamma_2 \delta_2 \varepsilon_1^4}{\varepsilon \varepsilon_1^4 \varepsilon_2^4}, \tag{17}$$

$$\xi_2 \equiv \frac{\gamma_1 \varepsilon_2^6 (\varepsilon_1^2 - 4\delta_1^2) + \gamma_2 \varepsilon_1^6 (\varepsilon_2^2 - 4\delta_2^2)}{\varepsilon \varepsilon_1^6 \varepsilon_2^6} + 4\xi_1^2, \tag{18}$$

$$\xi_3 \equiv \frac{42}{5} a_5 q_1 (\gamma_1 + \gamma_2)^2 \frac{2q_1^2 (\gamma_1 + \gamma_2) - \varepsilon \varepsilon_1^2 \varepsilon_2^2}{\varepsilon^3 \varepsilon_1^8 \varepsilon_2^8}, \tag{19}$$

$$\xi_4 \equiv -8\varepsilon \gamma_1 \gamma_2 \frac{\Delta \delta (2q_1 \Delta \delta + \varepsilon_2^2 - \varepsilon_1^2)}{(\gamma_1 + \gamma_2)^3 a_5} \xi_3. \tag{20}$$

Therefore, the expression we have obtained for the thermoelectric power can be viewed as a product involving the factor $-2|e| \mathcal{L}_0 T$, exhibiting a linear temperature dependence, and the auxiliary function defined by Eq. (16). This function exhibits a marked nonlinear temperature dependence. In the next section, we will account for some of the Seebeck coefficient anomalies reviewed in Sec. II by means of Eq. (15). To this end, we will focus on the main topological features of function $\mathcal{F}(T)$ and the physical implications of the parameters ξ_n .

V. DISCUSSION

A. Deviation from the linear behavior

In the low-temperature regime, the thermoelectric power of QC's belonging to the i -AlCu(Fe, Ru, Os) and i -AlPd(Mn, Re) families exhibit a linear dependence with T . At temperatures above ~ 50 – 100 K, however, the $S(T)$ curve clearly deviates from the linear behavior, exhibiting pronounced curvatures. This behavior can be readily described by means of Eqs. (15) and (16). In fact, since $\mathcal{F}(T \rightarrow 0) = \xi_1$, in the low-temperature limit Eq. (15) reduces to the linear form

$$S(T \rightarrow 0) = -2|e| \mathcal{L}_0 \xi_1 T \equiv aT. \tag{21}$$

The sign of the slope a is determined by the sign of the parameter ξ_1 which, in turn, depends on the electronic structure of the sample according to Eq. (17). The slope value is determined by two contributions: one involving universal constants only (whose value will be the same for all the samples); and a sample-dependent one given by the $|\xi_1|$ value. In order to gain some physical insight about the coefficient ξ_1 we will take the logarithm derivative of Eq. (1), obtaining the relationship

$$\xi_1 = \frac{1}{2} \left(\frac{d \ln \sigma(E)}{dE} \right)_{E=\mu}. \tag{22}$$

Therefore, Eq. (21) reduces to the well-known Mott's formula $S = -|e| \mathcal{L}_0 [d \ln \sigma(E) / dE]_{E=\mu} T$ in the low-temperature limit. In several previous works the validity of such an expression has been assumed for QC's in order to discuss some experimental results.^{28–30,35} From Eqs. (21) and (22) it follows that Mott's formula will properly describe the thermoelectric power of QC's as far as the remaining coefficients ξ_2 , ξ_3 , and ξ_4 in the $\mathcal{F}(T)$ function given by Eq. (16) are negligible as compared to ξ_1 . Since these coefficients are multiplied by the temperature-dependent factors bT^2 and b^2T^4 , respectively, it is clear that the range of validity of Eq. (21) will be strongly dependent on the electronic structure of the sample. We can quantitatively express this relationship by means of Eqs. (17)–(20), determining the corresponding ξ_n values.

B. Thermopower sign reversal

According to Eqs. (15) and (16), the overall sign of the thermoelectric power depends on the sign of the auxiliary function $\mathcal{F}(T)$ which, in turn, is determined by the electronic structure through the signs adopted by each ξ_n coefficient. In order to get a Seebeck coefficient sign reversal the condition $\mathcal{F}(T) \equiv 0$ should be satisfied. Thus, the $S(T)$ curve will have a crossing point at the temperature given by the relationship

$$T_0 = \sqrt{-\frac{\xi_1}{b \xi_3}}. \tag{23}$$

Therefore, the necessary condition for the existence of such a crossing point is that the coefficients ξ_1 and ξ_3 have opposite signs. This condition explains why not all samples exhibit such sign reversal. Equation (23) also defines two singular

TABLE I. Experimental values of the low-temperature thermopower slope a and sign reversal temperature T_0 for different QC's (taken from the literature), along with the corresponding values for the phenomenological coefficients ξ_1^{exp} and ξ_3^{exp} as determined from Eqs. (24) and (25). The values labeled (*) have been extrapolated from experimental curves in the range 4–300 K.

Reference	Sample	a ($\mu\text{V K}^{-2}$)	T_0 (K)	ξ_1^{exp} [(eV) $^{-1}$]	ξ_3^{exp} [(eV) $^{-3}$]
31	Al ₆₃ Cu ₂₅ Fe ₁₂	−0.39	398*	+8.02	−2078
26	Al ₆₅ Cu ₂₀ Ru ₁₅	−0.30	162	+6.09	−9557
26	Al ₆₈ Cu ₁₇ Ru ₁₅	−0.25	329*	+5.03	−1908
27	Al _{62.5} Cu ₂₅ Fe _{12.5}	−0.23	334*	+4.76	−1746
26	Al ₇₀ Cu ₁₅ Ru ₁₅	−0.22	285	+4.45	−2253
30	Al _{62.5} Cu ₂₅ Fe _{12.5}	−0.19	349	+3.85	−1294
29	Al _{64.5} Cu ₂₀ Ru ₁₅ Si _{0.5}	−0.07	197	+1.46	−1531

electronic structures, corresponding to the cases $\xi_1 = 0 \Rightarrow T_0 = 0$, and $\xi_3 = 0 \Rightarrow T_0 \rightarrow \infty$. In both cases we have no crossing points either.

According to Eq. (21) the coefficient ξ_1 can be obtained from the slope of the $S(T)$ curve in the low-temperature regime as

$$\xi_1^{\text{exp}} \approx -20.5a[\mu\text{V K}^{-2}], \quad (\text{eV})^{-1}. \quad (24)$$

Then, making use of Eqs. (21) and (23) the coefficient ξ_3 can be obtained from the experimental $S(T)$ curves by means of the relationship

$$\xi_3^{\text{exp}} \approx 8.4 \times 10^8 \left(\frac{a[\mu\text{V K}^{-2}]}{T_0} \right), \quad (\text{eV})^{-3}. \quad (25)$$

For the sake of illustration, in Table I we list the low-temperature thermopower slopes and T_0 values for some representative QC's, along with the corresponding values for the parameters ξ_1^{exp} and ξ_3^{exp} as determined from Eqs. (24) and (25). From the listed data we can appreciate that all QC's exhibiting thermopower sign reversals also exhibit negative slopes in the low-temperature regime. According to Eq. (21) this implies that ξ_1 takes on positive values in all the considered samples. Now, according to Eq. (22) we can express $\xi_1 = \sigma'(\mu)/2\sigma(\mu)$, so that the spectral conductivity will be a growing function around the Fermi level. Since the $\sigma(\mu)$ value can be experimentally measured by means of several techniques, we see that the study of the phenomenological coefficient ξ_1 provides us with a useful tool to obtain quantitative information about the spectral conductivity growth rate around the Fermi level from suitable experimental transport data.

C. Seebeck coefficient extrema

One of the most intriguing anomalies observed in the experimental thermopower data refers to the presence of extrema in both $S(T)$ and $S(T)/T$ curves. According to Eq. (15), relevant information on the auxiliary function $\mathcal{F}(T)$ can be directly obtained from the study of the experimental curve $S(T)/T$.^{30,39,40} To this end, we shall express Eq. (15) in the way

$$\mathcal{F}(T) \approx -20.5 \left(\frac{S[\mu\text{V K}^{-1}]}{T} \right), \quad (\text{eV})^{-1}. \quad (26)$$

On the other hand, by imposing the extrema condition $d\mathcal{F}(T)/dT = 0$ to Eq. (16) we obtain $T_1^0 = 0$, and

$$bT_1^2 = -\frac{\xi_1}{\xi_3} \pm \sqrt{\left(\frac{\xi_1}{\xi_3}\right)^2 + \frac{\xi_3 - \xi_1 \xi_2}{\xi_3 \xi_4}}. \quad (27)$$

Therefore, depending on the actual values of the ξ_n coefficients, two nontrivial extrema may be present in the $S(T)/T$ curve, namely, a maximum (minus sign choice) at T_1^- followed by a minimum (plus sign choice) at T_1^+ , ($T_1^- < T_1^+$). Quite interestingly, the presence of both extrema has been observed in a recent study of the i -MgZn(Y, Tb, Ho, Er) system, where a small hump in the $S(T)/T$ curve, at about $T_1^- \approx 15$ K, followed by a little dip at $T_1^+ \approx 50$ K, has been reported in all the considered samples.³⁹ The possible magnetic origin of such a hump can be ruled out as the hump also appears in the thermoelectric power of the nonmagnetic i -ZnMgY,⁴⁰ hence favoring an electronic structure origin for this feature. By mutually adding the solutions given by Eq. (27) we obtain the relationship

$$-\frac{\xi_1}{\xi_3} = \frac{b}{2} [(T_1^-)^2 + (T_1^+)^2], \quad (28)$$

and plugging the above experimental values for T_1^+ in Eq. (28) we obtain $\xi_1/\xi_3 \approx -3.3 \times 10^{-5}$ (eV) $^{-2}$. This figure is almost two orders of magnitude lower than that listed in Table I. This suggests that substantial differences among the electronic structure of i -AlCu(Fe, Ru) samples and the rare-earth bearing QC's should exist, in agreement with recent band-structure calculations.⁶⁴ Let us now consider the case of samples exhibiting a crossing temperature T_0 . In this case, we can make use of Eq. (23) to rewrite Eq. (27) in the form

$$bT_1^2 = bT_0^2 \pm \xi_4^{-2} \sqrt{1 + \xi_2 b T_0^2 + \xi_4 b^2 T_0^4}. \quad (29)$$

Then, taking into account Eq. (16) we obtain

$$bT_1^2 = bT_0^2 \pm \xi_4^{-2} \sqrt{\frac{\xi_1 + \xi_3 b T_0^2}{\mathcal{F}(T_0)}}, \quad (30)$$

and by mutually subtracting these solutions we get

$$\xi_4 = \left[\frac{-8}{|b|e} \frac{T_0}{S(T_0)} \frac{\xi_1 + \xi_3 b T_0^2}{[(T_1^+)^2 - (T_1^-)^2]^2} \right]^{1/4}. \quad (31)$$

This expression allows us to determine the coefficient ξ_4 value from the knowledge of the experimental data T_0 , T_1^\pm , and $S(T_0)$, provided that the values of ξ_1 and ξ_3 are known from Eqs. (24) and (25), respectively.

TABLE II. Systematic variation of the average electronic valence n , the electronic structure model parameters δ_i , and the phenomenological coefficients ξ_n , determined from Eqs. (17)–(20), as a function of the sample stoichiometry. ($\gamma_1 = 1.35$ eV, $\gamma_2 = 0.04$ eV).

Sample	n	$\Delta\mu$ (eV)	δ_1 (eV)	δ_2 (eV)	ξ_1 [(eV) $^{-1}$]	ξ_2 [(eV) $^{-2}$]	ξ_3 [(eV) $^{-3}$]	ξ_4 [(eV) $^{-4}$]
Al _{62.5} Cu _{24.5} Fe ₁₃	1.8015	−0.06	−0.381	+0.049	−11.45	+197	+1158	+15 039
Al ₆₂ Cu _{25.5} Fe _{12.5}	1.8088	−0.03	−0.406	+0.024	−10.63	+426	+710	+16 815
Al _{62.5} Cu ₂₅ Fe _{12.5}	1.8188	0.00	−0.440	−0.010	+5.73	+569	−1634	−50 573
Al ₆₃ Cu ₂₅ Fe ₁₂	1.8460	+0.09	−0.533	−0.103	+7.10	+32	−449	−2453
Al _{62.5} Cu _{26.5} Fe ₁₁	1.8705	+0.18	−0.617	−0.187	+3.38	−4	−47	−98

Finally, we will consider the presence of extrema in the $S(T)$ curve. To this end, we impose to Eq. (15) the extreme condition $dS(T)/dT = 0$ to get

$$\xi_3 \xi_4 y^3 + (3 \xi_1 \xi_4 - \xi_2 \xi_3) y^2 + (\xi_1 \xi_2 - 3 \xi_3) y - \xi_1 = 0, \quad (32)$$

where $y \equiv bT^2$. By means of Eq. (32), the possible existence of maxima or minima in the $S(T)$ curve can be related to the electronic structure in a precise, although somewhat involved way. In fact, Eq. (32) depends on all the phenomenological coefficients ξ_n . This fact helps us to understand the physical reasons motivating the strong dependence of these extrema on minor stoichiometric changes since by changing the electronic structure of the sample we are substantially modifying the values of the ξ_n coefficients which determine the solutions of Eq. (32).

D. Sample stoichiometry-dependence effects

The sensitivity of the thermopower curves to minor changes in the sample composition can be related to systematic changes of the electronic structure by means of Eqs. (15) and (16). To illustrate this point we shall consider the systematic variation of $S(T)$ for a series of i -AlCuFe QC's whose average electronic valence (number of electrons per atom) is modified by means of a systematic stoichiometric change. For a sample of general composition Al _{x} Cu _{y} Fe _{$1-x-y$} , the average valence is obtained from the expression $n = xn_{Al} + yn_{Cu} + (1-x-y)n_{Fe}$, where $n_{Al} = 3$, $n_{Cu} = 1$, and we have adopted the effective valence of $n_{Fe} = -2.45$ for the iron atoms. This value has been determined from sp - d hybridization effects in the tetragonal quasicrystalline approximant Al₇Cu₂Fe.^{67,68} From the knowledge of the average valence we can estimate the shift in the Fermi level by means of the relationship²⁹

$$\Delta\mu \approx 6.235 \times \frac{n_0 - n}{n_0}, \quad (\text{eV}), \quad (33)$$

where n_0 is a suitable reference value. In our case, we will take the sample Al_{62.5}Cu₂₅Fe_{12.5} as a reference one,²³ yielding $n_0 = 1.8188$ electrons per atom. Making use of Eqs. (33) and (17)–(20) we obtain the δ_i and ξ_n values listed in Table II for different i -AlCuFe samples. The influence of the stoichiometry in the electronic structure is shown in Fig. 2, where we clearly appreciate a progressive shift of the dip position in the spectral conductivity curve $\sigma(E)$. This shift correlates with the stoichiometry of the sample, leading to a systematic shift of the Fermi level given by $\Delta\mu$ in Table II. By plugging the phenomenological coefficients' values listed

in Table II into Eqs. (23) and (32) we can calculate the corresponding sign reversal and extrema temperatures. In Table III, we list the obtained results and compare them with suitable experimental data reported in the literature. Comparing the results presented in Fig. 2 and Tables II and III several conclusions can be drawn. First, we appreciate a good agreement between the measured and calculated T_0 and T_2 values for the Al_{62.5}Cu₂₅Fe_{12.5} and Al_{62.5}Cu_{24.5}Fe₁₃ samples. On the contrary, there exists a significant discrepancy between these values for the Al₆₃Cu₂₅Fe₁₂ sample. Such a difference is not surprising since the assumption of identical γ_1 and γ_2 values for all the considered samples seems very rough. Second, we observe that all the samples should exhibit a thermopower sign reversal (the phenomenological parameters ξ_1 and ξ_3 shown in Table II have opposite signs), although the corresponding crossing temperatures take values within a wide temperature range extending from 400 to 1700 K, approximately. Analogously, all the samples exhibit an extremum at a temperature whose value ranges from about 240 to 1200 K. In this regard, we should note the absence of an experimental confirmation for the predicted maximum at $T_2 \approx 237$ K for the Al₆₂Cu_{25.5}Fe_{12.5} sample. This absence should also be interpreted as indicating that more adequate values for the model parameters γ_1 and γ_2 may be taken into account. Third, there exists a clear correlation between the average electronic valence n , and the maximum (minimum) $S(T_2)$ value, as it can be readily seen by comparing Table III and Fig. 2. In fact, for those samples whose Fermi level is located between both Lorentzian features ($\delta_1 < 0, \delta_2 > 0$) the thermoelectric power exhibits a maximum [$S(T_2) > 0$]. Con-

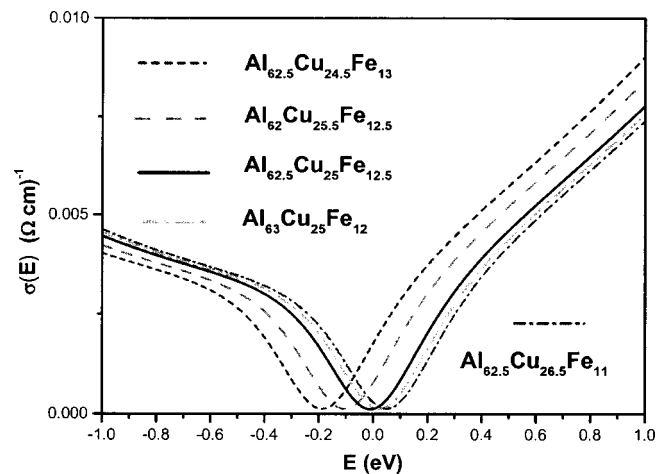


FIG. 2. Systematic variation of the spectral conductivity around the Fermi level as a function of the sample stoichiometry.

TABLE III. Comparison between the sign reversal. T_0 and extrema T_2 and $S(T_2)$ values obtained from the analytical expressions Eqs. (23) and (32) and some suitable experimental values reported in the literature. The values labeled (*) have been extrapolated from the experimental curve in the range 4–300 K.

Sample	T_0 (K)	T_0^{exp} (K)	T_2 (K)	T_2^{exp} (K)	$S(T_2)$ ($\mu\text{V K}^{-1}$)	$S(T_2^{\text{exp}})$ ($\mu\text{V K}^{-1}$)	Reference
$\text{Al}_{62.5}\text{Cu}_{24.5}\text{Fe}_{13}$	636		260	235	+84	+45	27
$\text{Al}_{62}\text{Cu}_{25.5}\text{Fe}_{12.5}$	783		237		+68		31
$\text{Al}_{62.5}\text{Cu}_{25}\text{Fe}_{12.5}$	379	350	169	155	-28	-23	30
$\text{Al}_{62.5}\text{Cu}_{25}\text{Fe}_{12.5}$	379	335*	169	150	-28	-24	27
$\text{Al}_{63}\text{Cu}_{25}\text{Fe}_{12}$	805	400*	454	115	-95	-26	31
$\text{Al}_{63}\text{Cu}_{25}\text{Fe}_{12}$	805		454	200	-95	-22	69
$\text{Al}_{62.5}\text{Cu}_{26.5}\text{Fe}_{11}$	1710		1224		-126		27

versely, for those samples whose Fermi level is located above both Lorentzian features ($\delta_1, \delta_2 < 0$) the thermoelectric power exhibits a minimum [$S(T_2) < 0$]. In addition, as the Fermi level progressively shifts from the position it occupies in the $\text{Al}_{62.5}\text{Cu}_{24.5}\text{Fe}_{13}$ sample to that corresponding to the $\text{Al}_{62.5}\text{Cu}_{26.5}\text{Fe}_{11}$ sample the absolute value of the thermoelectric power progressively decreases from $S(T_2) \approx +85 \mu\text{V K}^{-1}$ up to $S(T_2) \approx -130 \mu\text{V K}^{-1}$. Therefore, merely changing the average electronic valence by less than 4%, a substantial variation of the thermoelectric power of more than two orders of magnitude can be obtained. In this regard, it is interesting to note that the obtained extrema values are quite large for metallic alloys, being comparable to those measured in some semiconductor materials. This fact spurs the interest of considering QC's as tentative thermoelectric materials.²²

Finally, in Fig. 3 we graphically summarize the main results obtained in this section by comparing the temperature dependence of the Seebeck coefficient corresponding to the considered $i\text{-AlCuFe}$ samples in the temperature range 1–500 K. The qualitative overall behavior of the different $S(T)$ curves compares fairly well with the experimental measurements reported in the literature (see the references given in Tables I and III). In this sense, our phenomenological treatment provides a *unified description of the thermoelectric power* for the five considered samples, properly describing

the main topological features present in the experimental curves over a broad temperature range. Notwithstanding this, quantitative differences between our analytical results and the experimental curves are expected due to the approximate knowledge of the electronic structure model parameters for most of the samples considered. These differences can also be related to experimental uncertainties due to the strong dependence of the transport properties on different heat treatments,^{30,33} the sample microstructure,³⁴ and possible oxidation and/or diffusion effects.³⁰

VI. CONCLUSIONS

In this work, we present a detailed analytical study of the thermoelectric power of icosahedral QC's, introducing a phenomenological framework aimed to relate the main topological features of the experimental $S(T)$ curves to certain characteristic features of the electronic structure of the samples. Within this context the analytically derived ξ_n coefficients can be regarded as phenomenological parameters containing information about the electronic structure of the sample. In fact, since the values of the ξ_n coefficients can *also* be determined from the analysis of the experimental $S(T)$ curves, we can obtain information about the spectral conductivity function from the topological features of the experimental transport curves. The first step will be to determine the values of the ξ_n from the main topological features of the experimentally obtained transport curves making use of the expressions obtained in Sec. V. The next step will be to determine the electronic model parameters γ_i , δ_i , and A , from the ξ_n theoretical values derived in Sec. IV. Nonetheless, due to the involved nature of the analytical expressions relating the phenomenological coefficients to the model parameters, this is a rather difficult task. Fortunately, even the partial knowledge of some phenomenological coefficients suffices to gain some physical insight onto certain relevant features of the electronic spectrum of the sample, as it has been illustrated in Secs. IV and V. On the other hand, the involved nature of the analytical expressions for the ξ_n coefficients suggests that the study of one transport coefficient alone will not suffice, in general, to get a detailed picture of the sample electronic structure. Therefore, one reasonably expects that a sharper view about the main electronic features of the considered QC samples would ultimately emerge from the simultaneous measurement of different transport coefficients. In fact, preliminary results from a combined study of the analytical expressions for the $\sigma(T)$ and $S(T)$

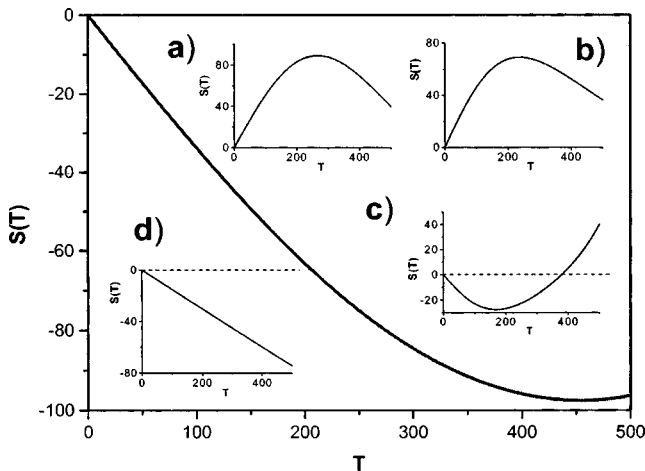


FIG. 3. Temperature dependence of the Seebeck coefficient in the temperature range 1–500 K for different sample compositions: $\text{Al}_{62.5}\text{Cu}_{24.5}\text{Fe}_{13}$ (a); $\text{Al}_{62}\text{Cu}_{25.5}\text{Fe}_{12.5}$ (b); $\text{Al}_{62.5}\text{Cu}_{25}\text{Fe}_{12.5}$ (c); $\text{Al}_{62.5}\text{Cu}_{26.5}\text{Fe}_{11}$ (d); and $\text{Al}_{63}\text{Cu}_{25}\text{Fe}_{12}$ (main frame).

curves indicates the convenience of such a procedure.⁷⁰ In this sense, measurements of the Seebeck coefficient in the regime of high temperatures would be very interesting as well. Finally, the phenomenological approach presented in this work may be straightforwardly extended to other systems whose electronic structure around the Fermi level is characterized by two main peaks separated by a well-defined pseudogap centered at the Fermi level. This includes a broad class of candidate materials for thermoelectric applications like Heusler-type alloys,⁷¹ hence widening the interest of our proposed framework for studying other structurally complex alloy phases of potential technological interest.

ACKNOWLEDGMENTS

The author warmly thanks C. Berger, J. M. Dubois, R. Escudero, T. Grenet, P. Häussler, C. Landauro, U. Mizutani, S. Roche, Z. M. Stadnik, and P. A. Thiel for interesting conversations and for sharing useful materials. The author acknowledges K. Giannò, A. L. Pope, and T. M. Tritt for sharing information and M. V. Hernández for a critical reading of the manuscript. This work is supported by the Consejería de Educación de la CAM and European Union FEDER through Project No. 07N/0070/2001.

- ¹A. P. Tsai, in *Physical Properties of Quasicrystals*, edited by Z. M. Stadnik, Springer Series in Solid-State Physics Vol. 126 (Springer-Verlag, Berlin, 1999), p. 5.
- ²E. Maciá, J. M. Dubois, and P. A. Thiel, *Ullmann's Encyclopedia of Industrial Chemistry*, (Wiley-VCH, Weinheim 2002); (6th ed., 2002 January Release on CD-ROM).
- ³Ö. Rapp, in Ref. 1, p. 127.
- ⁴S. Roche, G. Trambly de Laissardière, and D. Mayou, *J. Math. Phys.* **38**, 1794 (1997).
- ⁵J. S. Poon, *Adv. Phys.* **41**, 303 (1992).
- ⁶S. Legault, B. Ellman, J. O. Ström-Olsen, L. Taillefer, S. Kycia, T. Lograsso, and D. Delaney, in *New Horizons in Quasicrystals: Research and Applications*, edited by A. I. Goldman, D. J. Sordelet, P. A. Thiel, and J. M. Dubois (World Scientific, Singapore, 1997), p. 224.
- ⁷J. M. Dubois, S. S. Kang, P. Archembault, and B. Colletet, *J. Mater. Res.* **8**, 38 (1993).
- ⁸M. A. Chernikov, A. Bianchi, and H. R. Ott, *Phys. Rev. B* **51**, 153 (1995); P. A. Kalugin, M. A. Chernikov, A. Bianchi, and H. R. Ott, *ibid.* **53**, 14145 (1996); M. A. Chernikov, E. Felder, A. Bianchi, C. Wälti, M. Kenzelmann, H. R. Ott, K. Edagawa, M. de Boissieu, C. Janot, M. Feuerbacher, N. Tamura, and K. Urban, in *Proceedings of the 6th International Conference on Quasicrystals*, edited by S. Takeuchi and T. Fujiwara (World Scientific, Singapore, 1998), p. 451.
- ⁹K. Kiriwara and K. Kimura, *Sci. Tech. Adv. Materials* **1**, 227 (2000); R. Tamura, A. Waseda, K. Kimura, and H. Ino, *Phys. Rev. B* **50**, 9640 (1994).
- ¹⁰T. Klein, C. Berger, D. Mayou, and F. Cyrot-Lackmann, *Phys. Rev. Lett.* **66**, 2907 (1991).
- ¹¹A. Carlsson, *Nature (London)* **353**, 353 (1991).
- ¹²Z. M. Stadnik, D. Purdie, Y. Baer, and T. A. Lograsso, *Phys. Rev. B* **64**, 214 202 (2001); Z. M. Stadnik, in Ref. 3, p. 257.
- ¹³T. Klein and O. G. Symko, *Phys. Rev. Lett.* **73**, 2248 (1994).
- ¹⁴E. Maciá, *Appl. Phys. Lett.* **81**, 88 (2002).
- ¹⁵M. Krajić, J. Hafner, and M. Mihalkovič, *Phys. Rev. B* **62**, 024 205 (2001).
- ¹⁶Y. Ishii and T. Fujiwara, *Phys. Rev. Lett.* **87**, 206 408 (2001).
- ¹⁷R. Tamura, T. Asao, M. Tamura, and S. Takeuchi, *Mater. Res. Soc. Symp. Proc.* **643**, K13.3.1 (2001); R. Tamura, T. Asao, and S. Takeuchi, *Mater. Trans., JIM* **42**, 928 (2001).
- ¹⁸H. Sato, T. Takeuchi, and U. Mizutani, *Phys. Rev. B* **64**, 094 207 (2001); S. Takeuchi, T. Onogi, E. Banno, and U. Mizutani, *Mater. Trans., JIM* **42**, 933 (2001).
- ¹⁹P. Häussler, R. Haberken, C. Madel, J. Barzola-Quiquia, and M. Lang, *J. Alloys Compd.* **342**, 228 (2002); P. Häussler, H. Nowak, and R. Haberken, *Mater. Sci. Eng., A* **294–296**, 283 (2000); C. Roth, G. Schwalbe, R. Knöfler, F. Zavaliche, O. Madel, R. Haberken, and P. Häussler, *J. Non-Cryst. Solids* **252**, 869 (1999).
- ²⁰E. Maciá, *Phys. Rev. B* **61**, 8771 (2000).
- ²¹E. Maciá, *Appl. Phys. Lett.* **77**, 3045 (2000).
- ²²E. Maciá, *Phys. Rev. B* **64**, 094 206 (2001).
- ²³H. Solbrig and C. V. Landauro, *Physica B* **292**, 47 (2000); C. V. Landauro and H. Solbrig, *Mater. Sci. Eng., A* **294–296**, 600 (2000).
- ²⁴C. V. Landauro and H. Solbrig, *Physica B* **301**, 267 (2001).
- ²⁵J. L. Wagner, B. D. Biggs, and S. J. Poon, *Phys. Rev. Lett.* **65**, 203 (1990).
- ²⁶B. D. Biggs, S. J. Poon, and N. R. Munirathnam, *Phys. Rev. Lett.* **65**, 2700 (1990).
- ²⁷F. S. Pierce, S. J. Poon, and B. D. Biggs, *Phys. Rev. Lett.* **70**, 3919 (1993).
- ²⁸B. D. Biggs, Y. Li, and S. J. Poon, *Phys. Rev. B* **43**, 8747 (1991).
- ²⁹F. S. Pierce, P. A. Bancel, B. D. Biggs, Q. Guo, and S. J. Poon, *Phys. Rev. B* **47**, 5670 (1993).
- ³⁰R. Haberken, G. Fritsch, and M. Härting, *Appl. Phys. A: Solids Surf.* **57**, 431 (1993).
- ³¹A. Bilušić, D. Pavuna, and A. Smontara, *Vacuum* **61**, 345 (2001); A. Bilušić, A. Smontara, J. C. Lasjaunias, J. Ivkov, and Y. Calvayrac, *Mater. Sci. Eng., A* **294–296**, 711 (2000).
- ³²F. Giraud, T. Grenet, C. Berger, P. Lindqvist, C. Gignoux, and G. Fourcaudot, *Czech. J. Phys.* **46**, 2709 (1996).
- ³³T. M. Tritt, A. L. Pope, M. Chernikov, M. Feuerbacher, S. Legault, R. Cagnon, and J. Strom-Olsen, *Mater. Res. Soc. Symp. Proc.* **553**, 489 (1999); A. L. Pope, T. M. Tritt, M. Chernikov, M. Feuerbacher, S. Legault, R. Cagnon, and J. Strom-Olsen, *ibid.* **545**, 413 (1999).
- ³⁴A. L. Pope, T. M. Tritt, M. A. Chernikov, and M. Feuerbacher, *Appl. Phys. Lett.* **75**, 1854 (1999); A. L. Pope, R. Schneidmiller, J. W. Kolis, T. M. Tritt, R. Gagnon, J. Strom-Olsen, and S. Legault, *Phys. Rev. B* **63**, 052 202 (2001).
- ³⁵V. Fournée, U. Mizutani, T. Takeuchi, K. Saitoh, M. Ikeyama, J. Q. Guo, and A. P. Tsai, *Mater. Res. Soc. Symp. Proc.* **643**, K.14.3.1 (2001).
- ³⁶K. Giannò, A. V. Sologubenko, L. Liechtenstein, M. A. Chernikov, and H. R. Ott, *Ferroelectrics* **250**, 249 (2001).
- ³⁷R. Haberken, K. Khedhri, C. Madel, and P. Häussler, *Mater. Sci. Eng., A* **294–296**, 475 (2000).
- ³⁸K. Kiriwara, T. Nagata, and K. Kimura, *J. Alloys Compd.* **342**, 469 (2002).
- ³⁹K. Giannò, A. V. Sologubenko, M. A. Chernikov, H. R. Ott, I. R. Fisher, and P. C. Canfield, *Mater. Sci. Eng., A* **294–296**, 715 (2000).
- ⁴⁰A. L. Pope, T. M. Tritt, R. Gagnon, and J. Strom-Olsen, *Appl. Phys. Lett.* **79**, 2345 (2001).
- ⁴¹M. A. Howson and B. L. Gallagher, *Phys. Rep.* **170**, 265 (1988).
- ⁴²<http://virtual.clemson.edu/groups/TMRL/Papers/tmt/QCeoy99.pdf>.
- ⁴³K. Giannò (private communication).
- ⁴⁴P. A. Thiel and J. M. Dubois, *Nature (London)* **406**, 570 (2000).
- ⁴⁵S. Roche and D. Mayou, *Phys. Rev. Lett.* **79**, 2518 (1997).
- ⁴⁶See, for example, E. Maciá and F. Domínguez-Adame, *Electrons, Phonons, and Excitons in Low Dimensional Aperiodic Systems* (Editorial Complutense, Madrid, 2000).
- ⁴⁷E. Maciá and F. Domínguez-Adame, *Phys. Rev. Lett.* **76**, 2957 (1996), and references therein.
- ⁴⁸J. Friedel, *Helv. Phys. Acta* **61**, 538 (1988); T. Fujiwara and T. Yokokawa, *Phys. Rev. Lett.* **66**, 333 (1991).
- ⁴⁹U. Mizutani, *Mater. Trans., JIM* **42**, 901 (2001).
- ⁵⁰T. Klein, C. Berger, D. Mayou, and F. Cyrot-Lackmann, *Phys. Rev. Lett.* **66**, 2907 (1991).
- ⁵¹M. A. Chernikov, A. Bianchi, E. Felder, U. Gubler, and H. R. Ott, *Europhys. Lett.* **35**, 431 (1996).
- ⁵²M. Mori, S. Matsuo, T. Ishimasa, T. Matsuura, K. Kamiya, H. Inokuchi, and T. Matsukawa, *J. Phys.: Condens. Matter* **3**, 767 (1991).
- ⁵³E. Belin, Z. Dankhazi, A. Sadoc, Y. Calvayrac, T. Klein, and J. M. Dubois, *J. Phys.: Condens. Matter* **4**, 4459 (1992).
- ⁵⁴A. Shastri, F. Borsa, A. I. Goldman, J. E. Shield, and D. R. Torgeson, *J. Non-Cryst. Solids* **153 & 154**, 347 (1993); *Phys. Rev. B* **50**, 15 651 (1994).
- ⁵⁵T. Fujiwara, S. Yamamoto, and G. Trambly de Laissardière, *Phys. Rev. Lett.* **71**, 4166 (1993); G. Trambly de Laissardière and T. Fujiwara, *Phys. Rev. B* **50**, 5999 (1994); **50**, 9843 (1994).
- ⁵⁶J. Hafner and M. Krajić, in *Physical Properties of Quasicrystals*, edited by Z. M. Stadnik, Springer Series in Solid-State Physics Vol. 126 (Springer-Verlag, Berlin, 1999), p. 209.
- ⁵⁷C. Janot and M. de Boissieu, *Phys. Rev. Lett.* **72**, 674 (1994); C. Janot, *Phys. Rev. B* **53**, 181 (1996).

- ⁵⁸G. Trambly de Laissardière and D. Mayou, *Phys. Rev. B* **55**, 2890 (1997); G. Trambly de Laissardière, S. Roche, and D. Mayou, *Mater. Sci. Eng., A* **226–228**, 986 (1997).
- ⁵⁹Z. M. Stadnik and G. Stroink, *Phys. Rev. B* **47**, 100 (1993); G. W. Zhang, Z. M. Stadnik, A.-P. Tsai, and A. Inoue, *ibid.* **50**, 6696 (1994); A. Shastri, D. B. Baker, M. S. Conradi, F. Borsa, and D. R. Torgeson, *ibid.* **52**, 12 681 (1995).
- ⁶⁰Z. M. Stadnik, D. Pordie, M. Garnier, Y. Baer, A.-P. Tsai, A. Inoue, K. Edagawa, and S. Takeuchi, *Phys. Rev. Lett.* **77**, 1777 (1996); Z. M. Stadnik, D. Pordie, M. Garnier, Y. Baer, A.-P. Tsai, A. Inoue, K. Edagawa, S. Takeuchi, and K. H. J. Buschow, *Phys. Rev. B* **55**, 10 938 (1997).
- ⁶¹P. Lindqvist, P. Lanco, C. Berger, A. G. M. Jansen, and F. Cyrot-Lackmann, *Phys. Rev. B* **51**, 4796 (1995).
- ⁶²R. Escudero, J. C. Lasjaunias, Y. Calvayrac, and M. Boudard, *J. Phys.: Condens. Matter* **11**, 383 (1999).
- ⁶³T. Klein, O. G. Symko, D. N. Davydov, and A. G. M. Jansen, *Phys. Rev. Lett.* **74**, 3656 (1995); D. N. Davydov, D. Mayou, C. Berger, C. Gignoux, A. Neumann, A. G. M. Jansen, and P. Wyder, *ibid.* **77**, 3173 (1996).
- ⁶⁴M. Krajčí and J. Hafner, *J. Phys.: Condens. Matter* **12**, 5831 (2000).
- ⁶⁵E. S. Zijlstra and T. Janssen, *Europhys. Lett.* **52**, 578 (2000).
- ⁶⁶S. Roche and T. Fujiwara, *Phys. Rev. B* **58**, 11335 (1998).
- ⁶⁷G. Trambly de Laissardière, D. Mayou, and D. Nguyen Manh, *Europhys. Lett.* **21**, 25 (1993).
- ⁶⁸G. Trambly de Laissardière, D. Nguyen Manh, L. Magaud, J. P. Julien, F. Cyrot-Lackmann, and D. Mayou, *Phys. Rev. B* **52**, 7920 (1995).
- ⁶⁹F. Morales and R. Escudero, *Bull. Am. Phys. Soc.* **44**, 1276 (1999).
- ⁷⁰E. Maciá, *Phys. Rev. B* **66**, 174203 (2002).
- ⁷¹Y. Nishino, *Mater. Trans., JIM* **42**, 902 (2001).